ATR-FTIR Study of the Structure and Orientation of Transmembrane Domains of the *Saccharomyces cerevisiae* α-Mating Factor Receptor in Phospholipids†

Fa-Xiang Ding,‡ Haibo Xie,‡ Boris Arshava,‡ Jeffrey M. Becker,§ and Fred Naider*,‡

Department of Chemistry, The College of Staten Island of the City University of New York, Staten Island, New York 10314, and Department of Microbiology, University of Tennessee, Knoxville, Tennessee 37996

Received February 26, 2001; Revised Manuscript Received May 11, 2001

ABSTRACT: The structures of seven synthetic transmembrane domains (TMDs) of the α-factor receptor (Ste2p) from *Saccharomyces cerevisiae* were studied in phospholipid multilayers by transmission Fourier transform infrared (FTIR) and attenuated total reflection Fourier transform infrared (ATR-FTIR) spectroscopies. Peptide conformation assumed in multilayers depended on the method of sample preparation. Amide proton H/D exchange experiments showed that 60−80% of the NH bonds in these TMDs did not exchange with bulk water in 1,2-dimyristoyl-*sn*-glycero-3-phosphocholine (DMPC) multilayers. FTIR results showed that peptides corresponding to TMDs one, two, and seven were mostly α-helical in DMPC multilayers. Peptides corresponding to TMDs three and six assumed predominantly β-sheet structures, whereas those corresponding to TMDs four and five were a mixture of α-helices and β-sheets. ATR-FTIR showed that in DMPC the α-helices of TMDs two and five oriented with tilt angles of 34° and 32°, respectively, with respect to the multilayer normal. Similar results were obtained for six of the transmembrane domains in DMPC/DMPG (4:1) multilayers. In a mixture [POPC/POPE/POPS/PI/ergosterol (30:20:5:20:25)] which mimicked the lipid composition of the *S. cerevisiae* cell membrane, the percentage of α-helical structures found for TMDs one and five increased compared to those in DMPC and DMPC/DMPG (4:1) multilayers, and TMD six exhibited a mixture of β-sheet (∼60%) and α-helical (∼40%) structure. These experiments provide biophysical evidence that peptides representing the seven transmembrane domains in Ste2p assume different structures and tilt angles within a membrane multilayer.

The α-factor pheromone receptor (Ste2p) that is required for mating in the yeast *Saccharomyces cerevisiae* belongs to the large family of G protein-coupled receptors (GPCRs)[1] (*1, 2*). The receptor, like other GPCRs, contains seven transmembrane domains (TMDs) that are connected by intracellular and extracellular loops (*3, 4*). Biochemical studies indicate that ligand binding induces specific conformational changes in the TMDs (*5, 6*), which play key roles in transducing the signal across the plasma membrane (*1*). The elucidation of the conformational and orientational states of regions of the Ste2p receptor in membranes is crucial to reveal the molecular mechanism of ligand−receptor interaction and signal transduction. However, structural studies on such systems are hindered by the difficulty in obtaining crystals for X-ray diffraction and by restricted motion that makes them unsuitable for high-resolution solution NMR techniques. Studies on intact receptors are further stymied by their tendency to aggregate in solution.

Short fragments of receptors are amenable to biophysical analysis using circular dichroism (CD), nuclear magnetic resonance (NMR), and infrared (IR) techniques, and information concerning their structural tendencies has been shown to be relevant to the structure and function of the cognate integral membrane protein (*7*). Most important is the fact that fragments of receptors have been shown to spontaneously assemble into proteins which retain the biophysical and biological properties of the intact receptor (*8, 9*). Synthetic transmembrane domains of bacteriorhodopsin have been used to characterize the folding of this photoreceptor in phospholipid bilayers (*10*). Our recent CD study of the seven synthetic transmembrane domains of the α-factor receptor of *S. cerevisiae* showed that these receptor domains assumed α-helical structures in TFE/H_2O mixtures and two of the peptide domains formed β-sheet structures in sodium dodecyl sulfate micelles and dimyristoylphosphatidylcholine (DMPC) vesicles (*11*). Moreover, the secondary structure and the orientation of an 18-residue peptide corresponding to a portion of the 6th transmembrane domain of the α-factor receptor in DMPC multilayers have been measured and cross-checked by solid-state NMR and polarized attenuated total reflection infrared spectroscopy (ATR-FTIR) (*12*).

Infrared analysis has proven useful for studying the molecular conformation of peptides in lipid multilayer

† This work was supported by research grants GM22086 and GM22087 from the National Institutes of Health.

* Correspondence should be addressed to this author. Tel: (718)-9823896; Fax: (718)-9823910; email: naider@postbox.csi.cuny.edu.

‡ The College of Staten Island of the City University of New York.

§ University of Tennessee.

[1] Abbreviations: ATR-FTIR, attenuated total reflection Fourier transform infrared; CD, circular dichroism; DMPC, 1,2-dimyristoyl-*sn*-glycero-3-phosphocholine; DMPG, 1,2-dimyristoyl-*sn*-glycero-3-[phospho-*rac*-(1-glycerol)] sodium salt; GPCR, G protein-coupled receptor; HBTU, *O*-benzotriazolyl-*N*,*N*,*N*′,*N*′-tetramethyluronium hexafluorophosphate; HOBt, 1-hydroxybenzotriazole; MES, 2-(*N*-morpholino)ethanesulfonic acid; PI, phosphatidylinositol (sodium salt); POPC, 1-palmitoyl-2-oleoyl-*sn*-glycero-3-phosphocholine; POPE, 1-palmitoyl-2-oleoyl-*sn*-glycero-3-phosphoethanolamine; POPS, 1-palmitoyl-2-oleoyl-*sn*-glycero-3-[phospho-L-serine](sodium salt); SDS, sodium dodecyl sulfate; TFE, 2,2,2-trifluoroethanol; TMD, transmembrane domain.

10.1021/bi010394m CCC: $20.00
Published on Web 06/30/2001

environments (*13*−*22*). Previous studies have shown that ATR-FTIR gives information about lipid and protein orientation with respect to the axis that is perpendicular to the plane of the membrane (*22*−*28*). To carry out a comprehensive study on the parameters that influence the applicability of ATR-FTIR spectroscopy to fragments of membrane peptides, we have performed spectroscopic studies on the seven synthetic transmembrane domains of Ste2p bound to phospholipid multilayers. Herein we report on the influence of sample preparation, lipid, and peptide sequence on the structures assumed by these peptides.

EXPERIMENTAL PROCEDURES

Preparation of Lipid−*Peptide Vesicles for FTIR and ATR-FTIR.* Transmembrane domain peptides (ca. 0.13 mg in 0.13 mL of TFE) were added to 4 mg of DMPC, DMPC/DMPG (4:1), or POPC/POPE/POPS/PI/ergosterol (30:20:5:20:25) in 1 mL of $CHCl_3$. The resulting solution was dried under N_2 flow. Residual traces of organic solvent were removed by placing the dried film under vacuum overnight, and the lipid was suspended in 1 mL of 0.1 mM phosphate buffer, pH 6.3. The suspension was sonicated at approximately 50 °C for 60 min in a W-385 sonicator (Misonix, Inc., Farmingdale, NY) equipped with a cup horn (40% output power). The vesicle solution was exhaustively dialyzed into 600 mL of 0.1 mM phosphate buffer, pH 6.3, using Spectrapor 6 dialysis tubing with a 1000 molecular weight cutoff (VWR Scientific Products, Piscataway, NJ). The resulting vesicles were then passed through a 0.45 μm polycarbonate centrifugal filter. The calculated molar ratio of peptides to lipid was about 1:150.

Preparation of Lipid−*Peptide Vesicles for Fluorescence Studies.* The peptide (0.1 mg in 0.1 mL of TFE) was added to DMPC (10 mg in 0.5 mL of $CHCl_3$). The resulting solution was dried under N_2 flow. Residual traces of organic solvent were removed by placing the dried film under vacuum overnight, and the lipid was hydrated in 10 mL of 10 mM MES buffer, pH 6.3. The suspension was sonicated at approximately 50 °C for 60 min in a W-385 sonicator equipped with a cup horn at 40% output power. The resulting vesicles were then passed through a 0.45 μm polycarbonate centrifugal filter. The molar ratio of peptides to lipid was about 1:400.

FTIR and ATR-FTIR Spectroscopy. FTIR spectra were recorded at ambient temperature (~20 °C) on a Nicolet Magna 550 Fourier transform infrared spectrometer (Nicolet Analytical Instruments, Madison, WI) purged with N_2 and equipped with an DTGS detector and an ATR accessory (Pike Technologies, Inc., Madison, WI). The infrared beam was polarized using a 1 in. diameter wire-grid ZnSe polarizer. For each sample, 1000 interferograms were averaged at a spectral resolution of 4 cm^{-1} and processed using one-point zero-filling and Happ−Genzel apodization. For orientation studies, lipid films on the top surface of germanium ATR crystals (55 mm × 10 mm × 4 mm with 45° beveled edges) were obtained by slowly evaporating the vesicle solution (250 μL) in the presence or absence of peptides. The ATR crystals were previously cleaned with chloroform, TFE, and methanol, followed by 30 min plasma cleaning in a PDC-32G cleaner (Harrick, Ossining, NY). For transmission spectra, 100 μL of sample was dried on a CaF_2 window (25 mm diameter). Following deposition, the ATR crystals or CaF_2 windows were transferred to a desiccator where the films were rehydrated by vapor diffusion in an atmosphere maintained at 98% relative humidity using a saturated solution of K_2SO_4 in water (*29*). Rehydration was allowed to proceed for a minimum of 18 h at room temperature. The spectra for the respective phospholipid multilayers without peptide were subtracted to yield the difference spectrum of each peptide in the multilayer.

Peptide Amide H/D Exchange Experiment. One hundred microliters of the preformed lipid vesicle with or without peptide was dried on the surface of the CaF_2 window (25 mm diameter). The windows containing lipid films were rehydrated using the method described above. After FTIR spectra were recorded from the hydrated film, it was transferred to a drybox (i.e., an environment maintained at less than 10% relative humidity using P_2O_5), where it was dehydrated by storage at room temperature overnight. After recording FTIR spectra from the dry film in order to confirm dehydration, 8 μL of D_2O was added directly to its surface. The sample was tilted until the water had wet the entire surface of the film and then incubated in the dry environment for 30 min in order to allow most of the excess D_2O to evaporate. While some of the bulk D_2O was still visible on the surface of the film, it was transferred to a sealed chamber maintained at a relative humidity of 98% (in D_2O) by a saturated solution of K_2SO_4 in D_2O. The amide exchange was allowed to proceed 18 h. After all of the bulk D_2O had evaporated from the surface of the film, FTIR spectra of the samples were recorded in a N_2 environment.

Analysis of Orientation from ATR-FTIR Dichroism. Order parameters for the helical peptides were determined using established methods (*24*, *27*, *28*). The measured dichroic ratio, R^{ATR}, defined as the ratio between the absorption of light polarized parallel and perpendicular to the surface of the internal reflection element, was used to calculate an order parameter (S) using eq 1:

$$S = [(E_x^2 - R^{ATR}E_y^2 + E_z^2)/(E_x^2 - R^{ATR}E_y^2 - 2E_z^2)]/[(3\cos^2\alpha - 1)/2] \quad (1)$$

in which E_x, E_y, and E_z are the integrated absorption coefficients (*30*). If the film refractive index is independent of the wavelength, the above equation can be written in a simplified form, $E_x = 1.398$, $E_y = 1.516$, $E_z = 1.625$ (*25*):

$$S = [(R^{ATR} - 2)/(R^{ATR} + 1.45)]/[(3\cos^2\alpha - 1)/2] \quad (2)$$

where α is the angle between the principal transition dipole moment and the molecular director, $\alpha = 39°$ for the amide I mode (*24*). The order parameter S is related to the tilt angle β from the normal of the internal reflection element by the following equation:

$$S = (3\cos^2\beta - 1)/2 \quad (3)$$

Order parameters for the lipids are obtained from the symmetric and asymmetric stretching modes of the lipid methylene groups by setting $\alpha = 90°$.

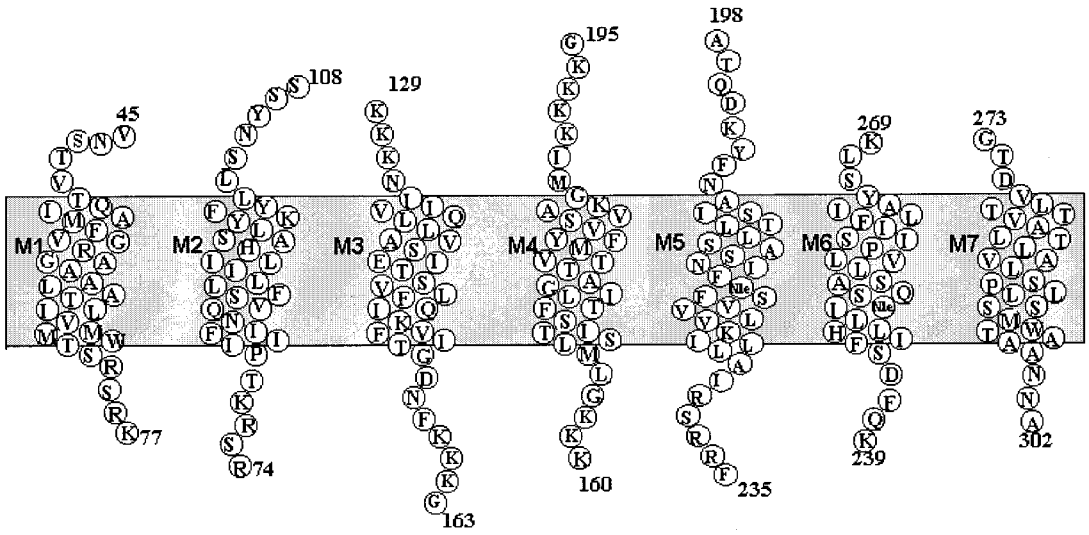

FIGURE 1: Cartoon illustrating synthetic peptides corresponding to the transmembrane domains of Ste2p. Sequences of domains are as follows: M1−33, VNSTVTQAIMFGVRAGAAALTLIVMWMTSRSRK; M2−35, RSRKTPIFIINQVSLFLIILHSALYFKYLLSNYSS; M3−35, KKKNIIQVLLVASIETSLVFQIKVIFTGDNFKKKG; M4−36, KKKGLMLTSISFTLGIATVTMYFVSAVKGMIKKKKG; M5−38, ATQDKYFNASTILLASSINFNleSFVLVVKLILAIRSRRF; M6−31, KQFDSFHILLINleSAQSLLVPSIIFILAYSLK; and M7−30, GTDVLTTVATLLAVLSLPLSSMWATAANNA. The underlined residues indicate changes from the wild-type sequence (see text).

The orientations, α and β, of β-sheet peptides relative to the membrane normal can be obtained from measurements of the dichroic ratios of two amide bands that have transition moments that are oriented parallel and perpendicular, respectively, to the strand axis by using eqs 4 and 5 (*31*):

$$R^{ATR}(\text{amide II}) = E_x^2/E_y^2 + 2(\cos^2\alpha)(\cos^2\beta)E_z^2/\{[1 - (\cos^2\alpha)(\cos^2\beta)]E_y^2\} \quad (4)$$

$$R^{ATR}(\text{amide I}) = E_x^2/E_y^2 + 2(\cos^2\alpha)(\sin^2\beta)E_z^2/\{[1 - (\cos^2\alpha)(\sin^2\beta)]E_y^2\} \quad (5)$$

where α is the angle by which the plane of the sheet is tilted to the membrane normal, and the strand axes are tilted at an angle β within the sheet, $(\sin^2\beta) = 1 - (\cos^2\beta)$; E_x, E_y, and E_z are the integrated absorption coefficients given above. By combining the dichroic ratios for both transition moment orientations, the sheet orientation, specified by $(\cos^2\alpha)$, and the strand orientation within the sheet, specified by $(\cos^2\beta)$, may be determined independently.

Fluorescence Spectroscopy. Fluorescence spectra were recorded using a photon-counting fluorometer (Fluoromax-3, SPEX, Edison, NJ) with a 1 × 1 cm quartz cuvette having a 2 mL sample volume. The sample was stirred using a magnetic bar until the spectrum was measured. The emission spectra were scanned between 300 and 420 nm with an excitation wavelength of 280 nm at intervals of 1 nm with 1 s integration time at each wavelength. Both the excitation and emission bandwidths were 3 nm.

Collisional Quenching Experiments. The lipid−peptide vesicle solution was stirred in a cuvette for half an hour. Fluorescence collisional quenching experiments with iodide were performed by adding increasing amounts of a 4 M KI solution in MES buffer [2-(*N*-morpholino)ethanesulfonic acid: 20 mM, pH 6.3] to a final concentration of 56 mM. Changes in fluorescence due to the addition of quencher were corrected by subtracting the fluorescence measured in a parallel DMPC vesicle control. The quenching of the fluorescence emission integrated from 320 to 380 nm was calculated with the Stern−Volmer equation:

$$F_0/F = 1 + K_{sv}[I^-] \quad (6)$$

where F_0/F is the ratio of fluorescence intensities in the presence of KCl and KI. The Stern−Volmer quenching constant, K_{sv}, was determined from the slope of F_0/F as a function of the iodide concentration, $[I^-]$.

RESULTS

Peptide Design and Reconstitution into Vesicles. Polypeptides corresponding to each of the seven transmembrane domains (see Figure 1 and accompanying legend for the structures of these peptides) in the native tertiary structure of α-factor receptor were chemically synthesized using solid-phase peptide chemistry on a Wang resin using α-Fmoc protection strategies and HBTU/HOBT activation (*11*, *32*, *33*). We designed the following polypeptides to include the entire transmembrane hydrophobic region plus some portion of the extracellular and cytoplasmic loops: M1−33(45−77, C59A) (in this abbreviation for peptide studied, M1 represents the first transmembrane domain predicted for Ste2p, 33 denotes the number of residues in the synthetic polypeptide, 45−77 are the residues of Ste2p contained in the peptide with residue 1 being the N-terminal residue of Ste2p, and C59A denotes a substitution of Ala in the synthetic peptide for Cys of the native Ste2p), M2−35(74−108), M3−35-(129−163, G129K, A130K, T131K, R161K, I162K), M4−36(160−195, R161K, I162K, V191K, T192K, Y193K, N194K, D195G), M5−38(198−235, M218Nle), M6−31-(239−269, M250Nle, C252A) (*32*), and M7−30(273−302) (*33*). It should be noted that M3−35 and M4−36 contain several additional flanking lysine residues added to both termini because peptides corresponding to the native sequence of the M3 and M4 transmembrane domains were almost insoluble and crude peptides could not be purified after exhaustive efforts. The native Cys residues in M1 and M6 were replaced with Ala to prevent disulfide formation

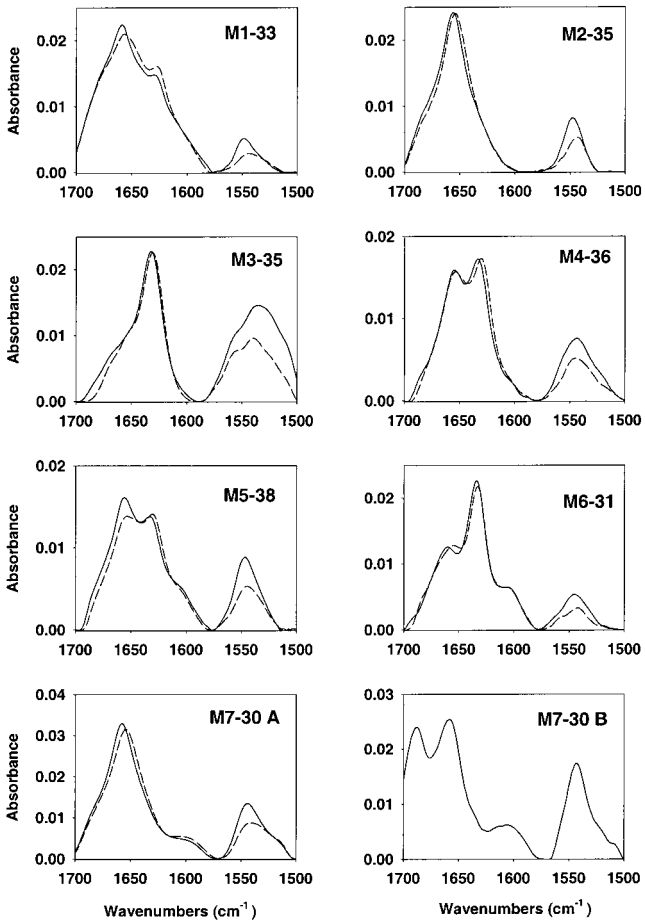

FIGURE 2: Amide I and amide II regions of the FTIR spectra of seven transmembrane domain peptides of Ste2p in phospholipid multilayers. Spectra were measured in DMPC multilayers hydrated in 98% H_2O relative humidity (solid line) or in 98% D_2O relative humidity (dashed line). For M7−30, spectra are shown for which DMPC vesicles were dialyzed and then dried on a CaF_2 window (M7−30 A) or for DMPC vesicles prepared without dialysis prior to drying on a CaF_2 window (M7−30 B).

during purification and biophysical studies. Ste2p with C59A and C252A substitutions exhibits full biological activity and pheromone binding (*8*). The Met residues in M5 and M6 were replaced by the isosteric Nle to prevent oxidation of Met during synthesis.

Reconstitution of the peptides into vesicles was achieved by sonication of peptide/DMPC, peptide/DMPC/DMPG (4:1), or peptide/POPC/POPE/POPS/PI/ergosterol (30:20:5:20:25) films in the presence of buffer followed by exhaustive dialysis of the vesicle suspension against buffer. It should be noted that the FTIR spectrum for the M7−30 sample, prepared by directly drying the vesicle suspension on the CaF_2 window prior to dialysis, exhibited a peak at 1688 cm^{-1} (Figure 2 , M7−30 B). The assignment of this band at 1688 cm^{-1} remains uncertain. It does not correspond to the vibration of the trifluoroacetate counterion that has been shown to exhibit a strong IR band around 1673 cm^{-1} (*34*, *35*), because this band did not appear when M6−18 (*12*), or M7−30 and M2−35 were dried on germanium crystals directly from TFE solution (data not shown). Previous studies have concluded that this band arises from an antiparallel β-sheet stucture (*36*−*41*). Interestingly, the peak at 1688 cm^{-1} disappeared (Figure 2, M7-30 A) after dialysis of the vesicle solution of M7−30. Similar results were obtained

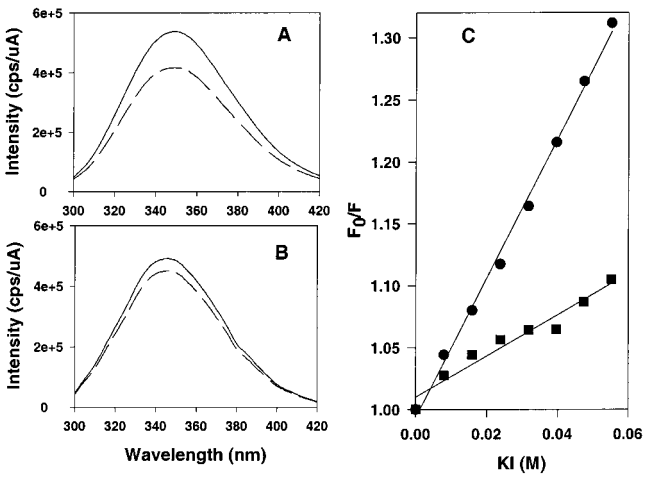

FIGURE 3: Fluorescence emission and quenching of M7−30 in the presence of KCl (50 mM, solid line) or KI (50 mM, dashed line). (A) Fluorescence emission of M7−30 in MeOH solution. (B) Fluorescence emission of M7−30 in the presence of DMPC vesicles. (C) Stern−Volmer plot of fluorescence quenching of M7−30 by KI in DMPC vesicles (■) and MeOH (●). Peptide concentration was 3.2 μM.

for several other transmembrane peptides (data not shown). Therefore, the method used to reconstitute the transmembrane peptides into vesicle is critically important. Since less complex spectra, as judged by the number of amide I components, were obtained after dialysis, the method described under Experimental Procedures (Preparation of Lipid−Peptide Vesicles for FTIR and ATR-FTIR) was used as a standard procedure in this paper.

Fluorescence Spectroscopy on Tryptophan-Containing Transmembrane Peptides. The analysis of the environment of membrane peptides can be assessed using fluorescence spectroscopy. Both M7−30 and M1−33 contain Trp residues that are predicted by hydropathy analysis to be in the hydrophobic interior of the lipid bilayer (see Figure 1). Fluorescence emission spectra of M7−30 in either DMPC vesicles or methanol solution were measured in the presence of KCl or KI (Figure 3). The emission λ_{max} of M7−30 is 345 nm in the presence of vesicles and 349 nm in methanol solution. The 4 nm blue shift indicates that the environment of the Trp residue in M7−30 is less polar in the vesicular preparation than that in methanol. The quenching experiment with KI indicates that the effect of this anion on the fluorescence intensity is greater in methanol than in the vesicle preparation (Figure 3A,B). The K_{sv} values for M7−30 in vesicles and methanol were determined directly from plots of F_0/F versus KI concentration (Figure 3C). Data were averaged from three independent measurements. K_{sv} of M7−30 in DMPC vesicles is 1.66 ± 0.13 M^{-1}, while K_{sv} of M7−30 in methanol is 5.64 ± 0.13 M^{-1}. Very similar results were obtained for M1−33 (*11*). These results showed that the accessibility of iodide anion to the indole groups of M7−30 or M1−33 in vesicles is lower than that in methanol. This supports the conclusion that the Trp residues in M7−30 and M1−33 are buried in the DMPC vesicle and shielded from iodide anion.

Secondary Structures of Seven TMDs in DMPC Multilayers. The correlation between the frequency of the amide I (primarily a carbonyl stretching mode) vibrational mode and the secondary structure of a polypeptide has been well

Table 1: Summary of Orientation Parameters and H/D Exchange Data for Ste2p TMDs in DMPC Multilayers

	M1−33	M2−35	M3−35	M4−36	M5−38	M6−31	M7−30
			Lipid				
R^{ATR} of CH_2 2919 (cm^{-1})[a]	1.08 ± 0.03	1.07 ± 0.01	1.12 ± 0.01	1.13 ± 0.02	1.10 ± 0.01	1.13 ± 0.03	1.05 ± 0.02
R^{ATR} of CH_2 2850 (cm^{-1})[a]	1.02 ± 0.01	1.02 ± 0.01	1.04 ± 0.02	1.07 ± 0.02	1.05 ± 0.01	1.08 ± 0.04	1.00 ± 0.00
S of lipid[b]	0.76 ± 0.04	0.77 ± 0.02	0.73 ± 0.04	0.71 ± 0.03	0.74 ± 0.03	0.71 ± 0.04	0.79 ± 0.04
tilt angle of lipid, β (deg)[c]	23 ± 2	24 ± 1	25 ± 2	26 ± 1	25 ± 2	26 ± 2	22 ± 2
			Peptides[d]				
amide I band (cm^{-1})	1658,1630	1656	1632	1655,1633	1656,1633	1633,1659	1658
amide II band (cm^{-1})	1548	1547	1536	1543	1547	1545	1544
amide II exchange (%)	32	36	42	34	34	42	24
R^{ATR} of amide I (II)[a]	1.82 ± 0.04	2.95 ± 0.25	2.43 ± 0.02 (2.04 ± 0.05)	1.87 ± 0.05	3.04 ± 0.25	2.10 ± 0.05 (1.67 ± 0.11)	2.29 ± 0.15
S of amide I[b]	−0.14 ± 0.04	0.53 ± 0.11		−0.10 ± 0.04	0.57 ± 0.10		0.19 ± 0.09
tilt angle of α-helix (β, deg) or β-sheet (α, deg)[c]	61 ± 2	34 ± 5	30 ± 2	59 ± 2	32 ± 4	39 ± 3	47 ± 3

[a] R^{ATR} of lipid is the dichroic ratio determined from the peak height of the CH_2 stretching absorption; R^{ATR} of amide I is the dichroic ratio integrated from 1650 to 1665 cm^{-1} for the α-helix and from 1628 to 1636 cm^{-1} for β-sheets; R^{ATR} of amide II is the dichroic ratio integrated from 1530 to 1540 cm^{-1} for M3−35 and from 1540 to 1550 cm^{-1} for M6−31. All R^{ATR} values represent averages from four independent measurements. [b] S is the order parameter calculated from the average dichroic ratio R^{ATR}. [c] See the text for details on the tilt angle calculations. [d] The lipid to peptide molar ratio was 150:1.

established in the literature (*42*). Frequencies in the region of 1650−1660 cm^{-1} correspond to α-helical segments while modes resonating in the regions of 1630−1640 and 1670−1685 cm^{-1} correspond to β-sheet elements. In DMPC, the M1−33, M2−35, and M7−30 peptides assume predominantly α-helical secondary structures with main amide I absorbances at approximately 1658, 1656, and 1658 cm^{-1}, respectively (Figure 2). A small shoulder at 1630 cm^{-1} for the amide I of M1−33 reflects a small amount of β-sheet. M3−35 and M6−31 were predominantly β-sheet structures with the main amide I absorbance at approximately 1632 and 1633 cm^{-1}, respectively. A shoulder at 1659 cm^{-1} for the amide I of M6−31 probably indicates a small amount of α-helix. In contrast to the above, M4−36 with amide I peaks at 1655 and 1633 cm^{-1} and M5−38 with amide I peaks at 1656 and 1633 cm^{-1} showed approximately equal mixtures of α-helical and β-sheet secondary structures in DMPC multilayers. These results are roughly consistent with the CD analysis on the same transmembrane domains of the α-factor receptor (*11*). It should be noted that random coil peptides such as α-helices have amide I absorbances between 1650 and 1660 cm^{-1} (*43*). However, the frequencies of the amide I regions were shifted less than 5 cm^{-1} during D_2O exchange experiments (Figure 2), indicating that the peptides have predominantly ordered structures in which the great majority of peptide bonds are involved in hydrogen bonds (*21, 44, 45*). Therefore, an unordered structure is not considered in our analysis.

Amide Proton H/D Exchange in Peptide/DMPC Multilayers. Amide proton H/D exchange occurs slowly in the hydrophobic environment of the multilayer since this would require disruption of the backbone hydrogen bonding pattern and exposure of the highly polar peptide bonds in an extremely hydrophobic environment (*46*−*48*). Thus, measurement of the extent of such exchange by observing the reduction in the amide II mode (a coupling of N−H rocking and C−N stretching modes) provides a reliable indication of the penetration of the peptide into the membrane (*44*). Accordingly, we used amide H/D exchange to estimate the percentage of the residues in the Ste2p receptor peptides which were protected by the DMPC multilayers.

The results from equivalent experiments on M1−33, M2−35, M3−35, M4−36, M5−38, M6−31, and M7−30 in DMPC multilamellar films are presented in Figure 2 and Table 1. For all the peptides, between 58% and 76% of the amide protons, corresponding to at least 20 residues in each peptide molecule, are protected from H/D exchange during an 18 h exposure of the peptides in phospholipid multilayers to 98% D_2O relative humidity. The protected residues must be participating in some kind of structural interaction which prevents their backbone protons from exchanging with bulk solvent. One interpretation is that significant proportions of all of the peptides were buried in the hydrophobic multilayers. Interestingly, there was little difference in the exchange rates for the peptides that were mostly α-helical compared to the peptides that were mostly β-sheet.

ATR-FTIR Spectroscopy of TMDs in DMPC Multilayers. FTIR spectroscopy of seven TMDs in DMPC multilayers showed that the secondary structures of M1−33, M2−35, and M7−30 were mostly α-helix, and those of M4−36 and M5−38 were a mixture of α-helical and β-sheet structures. Using polarized ATR-FTIR spectroscopy, it is possible to determine the orientation of the α-helical segments (*23*−*26, 42*), and β-sheet planes (*31*), with respect to the multilayer normal.

The orientations of the lipid chains of dry films in the presence of peptides were determined from the dichroism of the CH_2 stretching vibrations at 2850 cm^{-1} (symmetric) and 2919 cm^{-1} (asymmetric) in the ATR-FTIR absorbance spectra. The dichroic ratios averaged from four independent experiments were between 1.03 and 1.11 (Table 1). Assuming that the transition dipole moment of the symmetric CH_2 stretching vibration is perpendicular to the molecular axis, the resulting calculated order parameters, S, of the acyl chains were between 0.79 and 0.71, and the average tilt angles, β, of the lipid's CH_2 axis were between 22° and 26°, in agreement with the results for well-ordered fatty acid chains in the gel phase (*49*). These results indicate that the transmembrane domain peptides examined do not affect either the structure or the orientation of the multilamellar phase.

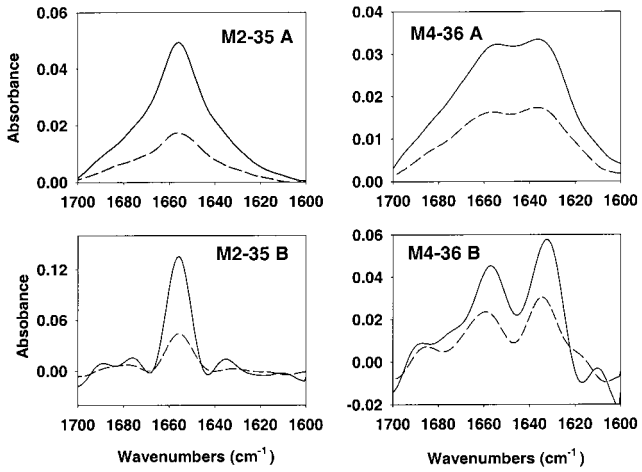

FIGURE 4: Amide I region of ATR-FTIR spectra of representative Ste2p TMDs in DMPC multilayers on Ge crystals. (A) Parallel (solid line) and perpendicular (dashed line) polarized light. (B) Fourier self-deconvoluted spectra of (A) using a bandwidth at half-height of 13 cm^{-1} and an enhancement of 2.0 (*50*).

ATR-FTIR spectra of the amide I regions were measured for M1−33, M2−35, M4−36, M5−38, and M7−30 in DMPC multilayers, and their Fourier self-deconvoluted spectra were calculated (see Figure 4 for representative spectra) (*50*). The dichroic ratios, R^{ATR}, calculated from the Fourier self-deconvoluted α-helical amide I vibrational regions integrated from 1650 to 1665 cm^{-1}, along with the respective order parameters *S* and tilt angles β, are summarized in Table 1. The dichroic ratio values, R^{ATR}, for M2−35 and M5−38 were calculated to be 2.95 and 3.04, respectively, resulting in corresponding order parameters of 0.53 and 0.57. These results indicate that helical regions of M2−35 and M5−38 orient at angles of 34° and 32°, respectively, between the axis of the α-helices and the multilayer normal. As the order parameter is influenced by both peptide orientation and multilayer order, the calculated angles represent maximum tilt angles, and it is likely that the tilt is actually lower. The dichroic ratio values, R^{ATR}, for M1−33, M4−36, and M7−30 were calculated to be 1.82, 1.87, and 2.29, respectively; the corresponding order parameters were −0.14, −0.10, and 0.19. These order parameter values were near the magic order parameter of 0. Therefore, in this case, we cannot distinguish whether these three peptides orient with maximum α-helix tilt angles of 61°, 59°, and 47° to the multilayer normal or whether they are disordered on the Ge surface. The dichroic ratios of M3−35 were measured to be 2.43 for the amide I region and 2.04 for the amide II region, and those of M6−31 were measured to be 2.10 for the amide I and 1.67 for the amide II, respectively (listed in Table 1). The tilt angles of β-sheet planes of M3−35 and M6−31 relative to the multilayer normal were calculated to be 30° and 39°, according to the method described under Experimental Procedures. Insertion of the β-sheet planes for M3−35 and M6−31 into the lipid multilayer was consistent with the similarities in the amide II H/D exchange rates for α-helical and β-sheet structure peptides. It should be noted that ATR-FTIR is evaluating an ensemble average of all α-helical or β-sheet structure amide bond orientations. To deconvolute the sample fractional order from the order parameter, site-directed infrared dichroism theory and selective labeling with ^{13}C have been developed to determine the tilt angle and pitch for specific residues in the M2 protein from influenza A virus (*50*−*52*), vpu protein from HIV-1 (*53*), and a model pentameric phospholamban (*54*). Given the complex nature of the IR results for the Ste2p TMDs, this approach might lead to additional insights into the structure of these peptides in DMPC multilayers.

ATR-FTIR Spectroscopy of TMDs in DMPC/DMPG Multilayers. DMPC vesicles have no net charge at the surface, while the transmembrane domains, especially M3−35 and M4−36 with two or three additional lysine residues at both ends, have positive charges. To address the question of whether the vesicle charge affects the conformation of the TMDs in phospholipid bilayers, we carried out ATR-FTIR spectroscopy of several TMDs in DMPC/DMPG (4:1) multilayers. For this study, we chose two peptides that were mostly α-helical in DMPC (M1−33 and M2−35), two mostly β-sheet peptides (M3−35 and M6−31), and two mixed α-helical and β-sheet peptides (M4−36 and M5−38). Of these materials, M3−35 and M4−36 have two or three additional positively charged residues at both the N and C termini. In this analysis, no attempt was made to determine the orientation of β-sheet-forming peptides.

As described above, the average tilt angles, β, of the lipid's CH_2 axis were determined to be between 23° and 30° (Table 2). These results, quite similar to those found in DMPC multilayers, showed that well-ordered DMPC/DMPG multilayers were also formed on the germanium surface. The amide I regions of ATR-FTIR spectra and their respective Fourier self-deconvoluted spectra for M1−33, M2−35, M4−36, M5−38, and M6−31 peptides in DMPC/DMPG (4:1) multilayers were measured, and the calculated R^{ATR}, *S*, and β values are summarized in Table 2. In this mixed lipid, M1−33 and M2−35 were still mostly α-helical, and M4−36 and M5−38 were mixtures of α-helix and β-sheet. M3−35 and M6−31 remained mostly β-sheet (data not shown). The content of α-helix for M4−36 significantly increased in a DMPC/DMPG (4:1) multilayer compared with that in a DMPC multilayer (compare Figure 5 with Figure 4). The α-helix tilt angles of those TMDs which were helical in a DMPC/DMPG multilayer are the same as those in DMPC multilayers, within experimental uncertainty. These results indicated that the conformation and orientation of the Ste2p TMDs are independent of the vesicle charge except that the negative charge at the DMPC/DMPG (4:1) bilayer surface increases the α-helical secondary structure for M4−36 which has extra positive charges at both ends. However, this effect cannot be generalized since M3−35, which also has extra positive charges at each terminus, remained predominantly β-sheet in a DMPC/DMPG (4:1) mixture.

ATR-FTIR Spectroscopy of TMDs in Mimetic Membrane Multilayers. ATR-FTIR spectra of six TMDs were measured in a membrane multilayer composed of a lipid composition which mimicked that of the yeast cell membrane (see Figure 6 for representative spectra). The dichroic ratios, R^{ATR}, and corresponding order parameters, *S*, and tilt angles, β, are summarized in Table 3. The results show that, in the membrane mimetic lipid mixture, M2−35 remains α-helical and M3−35 remains β-sheet (data not shown). M4−36 has the same proportion of α-helix and β-sheet as that in the DMPC multilayer. However, M1−33 had significantly more α-helix in membrane mimetic lipids than it had in DMPC

Table 2: Summary of Orientation Parameters for Ste2p TMDs in DMPC/DMPG (4:1) Multilayers

	M1−33	M2−35	M4−36	M5−38
		Lipid		
R^{ATR} of CH_2 2919 (cm^{-1})[a]	1.12 ± 0.03	1.10 ± 0.02	1.07 ± 0.01	1.08 ± 0.02
R^{ATR} of CH_2 2850 (cm^{-1})[a]	1.13 ± 0.04	1.05 ± 0.01	1.01 ± 0.01	1.01 ± 0.01
S of lipid[b]	0.67 ± 0.04	0.73 ± 0.02	0.77 ± 0.01	0.76 ± 0.03
tilt angle of lipid, β (deg)[c]	30 ± 4	25 ± 1	23 ± 1	24 ± 2
		Peptide[d]		
amide I band (cm^{-1})	1659,1632	1656	1656,1634	1653,1635
R^{ATR} of amide I band[a]	1.90 ± 0.06	2.96 ± 0.20	1.86 ± 0.15	3.16 ± 0.26
S of amide I band[b]	−0.07 ± 0.05	0.54 ± 0.10	−0.10 ± 0.13	0.63 ± 0.10
tilt angle of α-helix, β (deg)[c]	58 ± 2	34 ± 5	59 ± 6	30 ± 5

[a] R^{ATR} of lipid is the dichroic ratio determined from the peak height of the CH_2 stretching absorption; R^{ATR} of amide I is the dichroic ratio integrated from 1650 to 1665 cm^{-1}. All R^{ATR} values represent averages from four independent measurements. [b] S is the order parameter calculated from the average dichroic ratio R^{ATR}. [c] See the text for details on the tilt angle calculations. [d] The lipid to peptide molar ratio was 150:1.

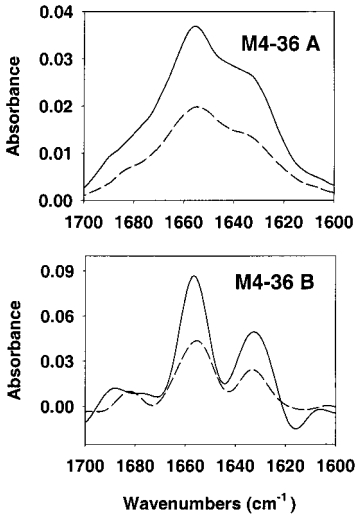

FIGURE 5: ATR-FTIR spectra of the amide I region of M4−36 in DMPC/DMPG (4:1) phospholipids on a germanium surface. (A) Parallel (solid line) and perpendicular (dashed line) polarized light. (B) Fourier self-deconvoluted spectra of (A) using a bandwidth at half-height of 13 cm^{-1} and an enhancement of 2.0 (*50*).

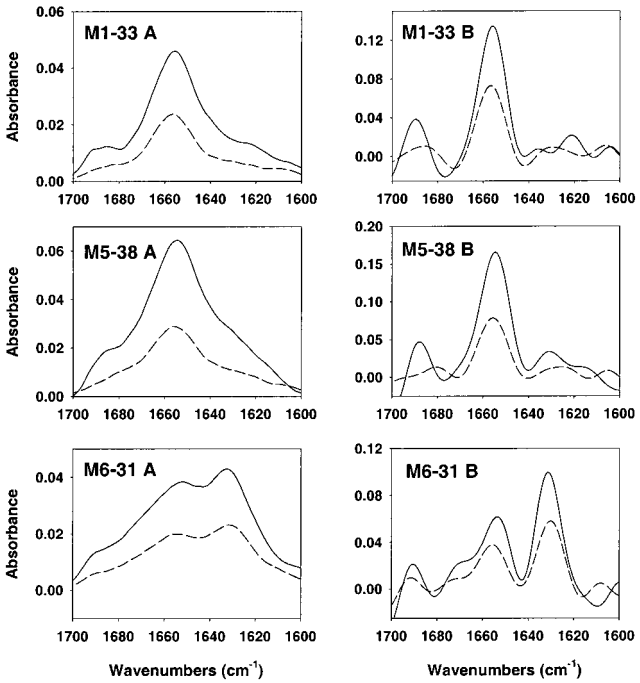

FIGURE 6: Analysis of Ste2p peptides in a membrane mimetic phospholipid mixture [POPC/POPE/POPS/PI/ergosterol (30:20:5:20:25)]. ATR-FTIR spectra of the amide I regions of dried M1−33, M5−38, and M6−31 peptides in POPC/POPE/POPS/PI/ergosterol (30:20:5:20:25) multilayers on a germanium surface. (A) Parallel (solid line) and perpendicular (dashed line) polarized light (B) Fourier self-deconvoluted spectra of (A) using a bandwidth at half-height of 13 cm^{-1} and an enhancement of 2.0 (*50*).

and DMPC/DMPG multilayers (Figure 6). Significantly, M5−38 had much more α-helix content, and M6−31 showed appreciable α-helical secondary structure as judged by the peak near 1660 cm^{-1}. We observed that the lipids of the mimetic membrane oriented poorly on the germanium surface with order parameters of 0.25 to 0.38 (Table 3). These disordered lipids resulted in disorder of the TMDs at the germanium surface in the mimetic membrane.

DISCUSSION

The goal of the present work was to use IR techniques to investigate the secondary structure and orientation of the seven transmembrane domains of Ste2p in phospholipid multilayers. FTIR results showed that peptides corresponding to TMDs one, two, and seven formed mostly α-helical structures and those corresponding to TMDs three and six formed mostly β-sheet structures, while domains four and five assumed nearly equal amounts of α-helical and β-sheet structures in DMPC multilayers. Amide II H/D exchange experiments revealed that most residues of the seven TMDs were shielded from bulk water and were likely buried in the apolar side chains of the DMPC multilayers. This conclusion was substantiated by fluorescence analysis of the only TMDs (M1−33 and M7−30) that contain Trp residues (Figure 3).

The qualitative results of the IR analysis and in particular the β-sheet structures assumed by M3−35 and M6−31 were fully consistent with previous CD studies in DMPC vesicles (*11*). However, the α-helical contents for TMDs M1−33, M2−35, M4−36, M5−38, and M7−30 differed somewhat from those determined by the CD analysis (*11*). The CD studies showed that the percentage of α-helix decreased in the order of M4 > M1 > M2 ≈ M5 > M7, whereas FTIR showed an α-helical content decreasing as follows: M2 ≈ M7 > M1 > M5 > M4. This observation indicates that when vesicles are slowly dried on CaF_2 windows or germanium plates to form multilayers, the interaction of the peptide segments with each other or with the phospholipid may differ from those in suspended vesicles.

Transmembrane domains are predicted to assume an α-helical secondary structure because this is the most stable

Table 3: Summary of Orientation Parameters for Ste2p TMDs in Mimetic Membrane Multilayers

	M1−33	M2−35	M4−36	M5−38	M6−31
		Lipid			
R^{ATR} of CH_2 2922 (cm^{-1})[a]	1.43 ± 0.09	1.47 ± 0.10	1.53 ± 0.06	1.58 ± 0.20	1.55 ± 0.14
R^{ATR} of CH_2 2853 (cm^{-1})[a]	1.47 ± 0.04	1.51 ± 0.04	1.40 ± 0.12	1.64 ± 0.22	1.52 ± 0.19
S of lipid[b]	0.38 ± 0.06	0.35 ± 0.06	0.36 ± 0.07	0.25 ± 0.14	0.31 ± 0.13
tilt angle of lipid, β (deg)[c]	40 ± 2	41 ± 2	41 ± 3	45 ± 5	43 ± 5
		Peptide[d]			
amide I band (cm^{-1})	1656	1657	1653,1629	1656	1652,1632
R^{ATR} of amide I band[a]	1.82 ± 0.01	2.07 ± 0.03	1.68 ± 0.02	2.12 ± 0.17	1.66 ± 0.11
S of amide I band[b]	−0.14 ± 0.01	0.05 ± 0.01	−0.25 ± 0.01	0.08 ± 0.11	−0.27 ± 0.10
tilt angle of α-helix, β (deg)[c]	61 ± 1	53 ± 1	66 ± 1	52 ± 5	67 ± 6

[a] R^{ATR} of lipid is the dichroic ratio determined from the peak height of the CH_2 stretching absorption; R^{ATR} of amide I is the dichroic ratio integrated from 1650 to 1665 cm^{-1}. All R^{ATR} values represent averages from four independent measurements. [b] S is the order parameter calculated from the average dichroic ratio R^{ATR}. [c] See the text for details on the tilt angle calculations. [d] The lipid to peptide molar ratio was 150:1.

structure in the hydrophobic interior of the lipid (*55*). Isolated β-strand structures in membranes would be especially high in energy due to un-hydrogen-bonded amide groups. Direct biophysical evidence for α-helices in a GPCR come from recent studies with rhodopsin, a photoreceptor (*56*−*58*). This elegant analysis showed that the seven transmembrane domains have different lengths, tilt angles, kinks, and regularities. Interestingly, the arrangement of the TMDs in rhodopsin differs significantly from those in bacteriorhodopsins. Unfortunately, due to the lack of good crystals, no direct structural information is available on other intact GPCRs.

Indirect information was obtained on receptors and transporters by studying model peptides corresponding to fragments of these integral membrane proteins. Results on fragments from rhodopsin indicate reasonable agreement between NMR structures found for a peptide corresponding to the seventh transmembrane domain and the crystal structure recently reported for the intact receptor (*59*). The seven transmembrane peptides of bacteriorhodopsin were previously subjected to detailed analysis using CD, FTIR, and proteolysis experiments (*10*). Peptides representing the first five transmembrane domains formed α-helical structures in detergent and lipids, whereas a peptide corresponding to the seventh transmembrane domain (BR-G) formed a hyperstable β-sheet structure (*10*). Five of the first six transmembrane peptides of the CFTR transporter were found to be helical whereas the sixth domain underwent a shift from an α-helix to a β-sheet structure in 20% methanol (*60*).

In the present study, two of the transmembrane peptides of Ste2p were shown to assume predominantly β-sheet structures in phospholipid multilayers. The finding of other than α-helical structures for the membrane peptides of bacteriorhodopsin, CFTR, and Ste2p suggests that model peptides may not be fully satisfactory as surrogates for the domains of the intact protein, and that long-range interactions must be taken into account to understand the folding and assembly of various domains of membrane proteins. This conclusion is consistent with the observation that the BR-G peptide of bacteriorhodopsin forms a β-sheet structure when studied alone but is known to be helical in the intact protein as judged by diffraction studies (*61*−*64*), and polarized FTIR analysis (*47*), and by FTIR analysis on a fragment of bacteriorhodopsin containing helices C through G of the receptor (*65*). These results allowed Engelman and coworkers to conclude that the sequence corresponding to the G helix of the photoreceptor can adopt very different conformations in different molecular contexts (*10*). Thus, although peptides are valuable models to investigate biophysical tendencies of regions of membrane proteins, one must be cautious in extending the results on isolated peptides to the intact protein. Alternatively, when spectroscopic analysis indicates that a model peptide may be α-helical under one set of conditions and assume a β-sheet structure when the conditions are changed, this finding may be biologically relevant. Specifically, such information may be indicative that in the native receptor the region modeled by the peptide is structurally flexible and is involved in the conformational changes thought to occur upon activation of signal transduction pathways. Only detailed X-ray analyses of the intact receptor in the active and inactive states can resolve this issue.

We observed that the method of sample preparation and the lipid used were very important in determining the conformational state of membrane peptides in DMPC multilayers. Direct sonication of several of the peptides in the presence of DMPC resulted in additional peaks in the amide I region of the FTIR spectrum (Figure 2). In contrast, when solutions of the sonicated peptides were equilibrated by dialysis, simpler FTIR spectra were obtained. The differences observed in the FTIR spectra of different sample preparations likely arise from conformational changes that occur during dialysis. We have not determined why these changes occur during dialysis and not during extensive sonication. However, one possibility is that the time (2 days during dialysis and 1 h maximum during sonication) is a factor. Electrostatic interactions between the cationic peptides and negatively charged membranes have been suggested to drive the peptide to bind to the membrane and form a stable helical structure (*17*, *18*). The secondary structures and α-helix orientations of M1−33, M2−35, and M5−38 were almost the same in zwitterionic DMPC multilayers as those in negatively charged DMPC/DMPG (4:1) multilayers. The α-helical content of M4−36 with six additional lysine residues at the two chain ends increased while the orientation remained the same. The results indicate that although peptide−lipid interactions were mostly governed by hydrophobic effects for M1−33, M2−35, and M5−38, electrostatic interaction between the negatively charged vesicles and positively charged M4−36 stabilized the α-helical conformation. Given the above observations, it is therefore important to consider conditions for sample preparation and lipid composition in

designing and interpreting ATR-FTIR experiments on fragments of integral membrane proteins.

This study reports the first ATR-FTIR experiments of synthetic Ste2p transmembrane domains in mutlilayers mimicking the composition of the *S. cerevisiae* cell membrane. We observed that the α-helical secondary structures of M1−33, M5−38, and M6−31 increased in the mimetic yeast membrane multilayers. Most significantly, M6−31 exhibited a mixture of β-sheet (∼60%) and α-helical (∼40%) structures. This represents the first experimental evidence that this peptide, which represents domain VI of Ste2p, can assume appreciable α-helical structure. The conformational diversity of this peptide has implications for the involvement of domain VI of Ste2p in a conformational change upon pheromone binding (*5*, *6*). Specifically, mutations in M6 of the full receptor have been reported to lock the receptor into the constitutively activated state (*66*, *67*). Thus, the conformational flexibility observed in peptides corresponding to M6 of Ste2p may play a key role in signal transduction. Whether the various structures assumed by the peptide fragments are maintained in the fully mature native receptor, and how these partial structures contribute to the folding of the receptor during biosynthesis and to receptor conformational change during signal transduction, will be interesting questions to pursue.

REFERENCES

1. Dohlman, H. G., Thorner, J., Caron, M. G., and Lefkowitz, R. J. (1991) *Annu. Rev. Biochem. 60*, 653−688.
2. Kurjan, J. (1992) *Annu. Rev. Biochem. 61*, 1097−1129.
3. Burkholder, A. C., and Hartwell, L. H. (1985) *Nucleic Acids Res. 13*, 8463−8475.
4. Bourne, H. R. (1997) *Curr. Opin. Cell Biol. 9*, 134−142.
5. Bukusoglu, G., and Jenness, D. D. (1996) *Mol. Cell. Biol. 16*, 4818−4823.
6. Dube, P., and Konopka, J. B. (1998) *Mol. Cell. Biol. 18*, 7205−7215.
7. Albert, A. D., and Yeagle, P. L. (2000) *Methods Enzymol. 315*, 107−115.
8. Martin, N. P., Leavitt, L. M., Sommers, C. M., and Dumont, M. E. (1999) *Biochemistry 38*, 682−695.
9. Ridge, K. D., Lee, S. S., and Yao, L. L. (1995) *Proc. Natl. Acad. Sci. U.S.A. 92*, 3204−3208.
10. Hunt, J. F., Earnest, T. N., Bousche, O., Kalghatgi, K., Reilly, K., Horvath, C., Rothschild, K. J., and Engelman, D. M. (1997) *Biochemistry 36*, 15156−15176.
11. Xie, H., Ding, F.-X., Schreiber, D., Eng, G., Liu, S.-F., Arshava, B., Arevalo, E., Becker, J. M., and Naider, F. (2000) *Biochemistry 39*, 15462−15474.
12. Valentine, K. G., Liu, S.-F., Marassi, F. M., Veglia, G., Opella, S. J., Ding, F.-X., Wang, S.-H., Arshava, B., Becker, J. M., and Naider, F. (2001) *Biopolymers* (in press).
13. Fahmy, K., Sakmar, T. P., and Siebert, F. (2000) *Biochemistry 39*, 10607−10612.
14. Abrecht, H., Goormaghtigh, E., Ruysschaert, J. M., and Homble, F. (2000) *J. Biol. Chem. 275*, 40992−40999.
15. Ghosh, J. K., Peisajovich, S. G., and Shai, Y. (2000) *Biochemistry 39*, 11581−11592.
16. Khurana, R., and Fink, A. L. (2000) *Biophys. J. 78*, 994−1000.
17. Oren, Z., and Shai, Y. (2000) *Biochemistry 39*, 6103−6114.
18. Hong, J., Oren, Z., and Shai, Y. (1999) *Biochemistry 38*, 16963−16973.
19. Han, X., Steinhauer, D. A., Wharton, S. A., and Tamm, L. K. (1999) *Biochemistry 38*, 15052−15059.
20. Arkin, I. T., Sukharev, S. I., Blount, P., Kung, C., and Brunger, A. T. (1998) *Biochim. Biophys. Acta 1369*, 131−140.
21. Corbin, J., Methot, N., Wang, H. H., Baenziger, J. E., and Blanton, M. P. (1998) *J. Biol. Chem. 273*, 771−777.
22. Bahng, M. K., Cho, N. J., Park, J. S., and Kim, K. (1998) *Langmuir 14*, 463−470.
23. Arkin, I. T., Rothman, M., Ludlam, C. F. C., Aimoto, S., Engelman, D. M., Rothschild, K. J., and Smith, S. O. (1995) *J. Mol. Biol. 248*, 824−834.
24. Arkin, I. T., Russ, W. P., Lebendiker, M., and Schuldiner, S. (1996) *Biochemistry 35*, 7233−7238.
25. Menikh, A., Saleh, M. T., Gariepy, J., and Boggs, J. M. (1997) *Biochemistry 36*, 15865−15872.
26. Sharon, M., Oren, Z., Shai, Y., and Anglister, J. (1999) *Biochemistry 38*, 15305−15316.
27. Smith, S. O., Jonas, R., Braiman, M., and Bormann, B. J. (1994) *Biochemistry 33*, 6334−6341.
28. Tamm, L. K., and Talulian, S. A. (1993) *Biochemistry 32*, 7720−7726.
29. Hunt, J. F., Rath, P., Rothschild, K. J., and Engelman, D. M. (1997) *Biochemistry 36*, 15177−15192.
30. Harrick, N. J. (1967) *Internal Reflection Spectroscopy*, Interscience Publisher, New York.
31. Marsh, D. (1997) *Biophys. J. 72*, 2710−2718.
32. Arshava, B., Liu, S.-F., Jiang, H., Breslav, M., Becker, J. M., and Naider, F. (1998) *Biopolymers 46*, 343−357.
33. Reddy, A. P., Tallon, M. A., Becker, J. M., and Naider, F. (1994) *Biopolymers 34*, 679−689.
34. Surewicz, W. K., and Mantsch, H. H. (1989) *J. Mol. Struct. 214*, 143−147.
35. Surewicz, W. K., Mantsch, H. H., and Chapman, D. (1993) *Biochemistry 32*, 389−394.
36. Krimm, S., and Bandekar, J. (1986) *Adv. Protein Chem. 38*, 181−364.
37. Chirgadze, Y. N., and Nevskaya, N. A. (1976) *Biopolymers 15*, 607−625.
38. Nabedryk, E., Garavito, R. M., and Breton, J. (1988) *Biophys. J. 53*, 671−676.
39. Jackson, M., Haris, P. I., and Chapman, D. (1989) *Biochim. Biophys. Acta 998*, 75−79.
40. Haris, P. I., and Chapman, D. (1995) *Biopolymers 37*, 251−263.
41. Harris, P. I., Lee, D. C., and Chapman, D. (1986) *Biochim. Biophys. Acta 874*, 255−265.
42. Braiman, M. S., and Rothschild, K. J. (1988) *Annu. Rev. Biophys. Biophys. Chem. 17*, 541−570.
43. Susi, H., Timasheff, S. N., and Stevens, L. (1967) *J. Biol. Chem. 242*, 5460−5466.
44. Baenziger, J. E., and Methot, N. (1995) *J. Biol. Chem. 270*, 29129−29137.
45. Baenziger, J. E., and Chew, J. P. (1997) *Biochemistry 36*, 3617−3624.
46. Zhang, Y. P., Lewis, R. N., Hodges, R. S., and McElhaney, R. N. (1992) *Biochemistry 31*, 11572−11578.
47. Earnest, T. N., Herzfeld, J., and Rothschild, K. J. (1990) *Biophys. J. 58*, 1539−1546.
48. Holloway, P. W., and Buchheit, C. (1990) *Biochemistry 29*, 9631−9637.
49. Nabet, A., Boggs, J. M., and Pezolet, M. (1994) *Biochemistry 33*, 14792−14799.
50. Kukol, A., Adams, P. D., Rice, L. M., Brunger, A. T., and Arkin, I. T. (1999) *J. Mol. Biol. 286*, 951−962.
51. Arkin, I. T., MacKenzie, K. R., and Brunger, A. T. (1997) *J. Am. Chem. Soc. 119*, 8973−8980.
52. Kukol, A., and Arkin, I. T. (2000) *J. Biol. Chem. 275*, 4225−4229.
53. Kukol, A., and Arkin, I. T. (1999) *Biophys. J. 77*, 1594−1601.
54. Torres, J., Adams, P. D., and Arkin, I. T. (2000) *J. Mol. Biol. 300*, 677−685.
55. Engelman, D. M., Steitz, T. A., and Goldman, A. (1986) *Annu. Rev. Biophys. Biophys. Chem. 15*, 321−353.
56. Schertler, G. F., Villa, C., and Henderson, R. (1993) *Nature 362*, 770−772.

57. Urger, V. M., and Schertler, G. F. (1995) *Biophys. J. 68*, 1776−1786.
58. Palczewski, K., Kumasaka, T., Hori, T., Behnke, C., Motoshima, H., Fox, B. A., Trong I. L., Teller, D. C., Okada, T., Stenkamp, R. E., Yamamota, M., and Miyano, M. (2000) *Science 289*, 739−745.
59. Yeagle, P. L., Danis, C., Choi, G., Alderfer, J. L., and Albert, A. D. (2000) *Mol. Vis. 6*, 125−131.
60. Wigley, W. C., Vijayakumar, S., Jones, J. D., Slaughter, C., and Thomas, P. J. (1998) *Biochemistry 37*, 844−853.
61. Pebay-Peyroula, E., Rummel, G., Rosenbusch, J. P., and Landau, E. M. (1997) *Science 277*, 1676−1681.
62. Kimura, Y., Vassylyev, D. G., Miyazawa, A., Kidera, A., Matsushima, M., Mitsuoka, K., Murata, K., Hirai, T., and Fujiyoshi, Y. (1997) *Nature 389*, 206−211.
63. Grigorieff, N., Ceska, T. A., Downing, K. H., Baldwin, J. M., and Henderson, R. (1996) *J. Mol. Biol. 259*, 393−421.
64. Teller, D. C., Okada, T., Behnke, C. A., Palczewski, K., and Stenkamp, R. E. (2001) *Biochemistry* (in press).
65. Earnest, T. N. (1987) *Fourier Transform Infrared and Resonance Raman Spectroscopic Studies of Bacteriorhodopsin*, Ph.D. Dissertation, Boston University, Boston, MA.
66. Sommers, C., Martin, N. P., Akal-Strader, A., Becker, J. M., Naider, F., and Dumont, M. E. (2000) *Biochemistry 39*, 6898−6909.
67. Konopka, J. B., Margarit, S. M., and Dube, P. (1996) *Proc. Natl. Acad. Sci. U.S.A. 93*, 6764−6769.

BI010394M